Open access • Journal Article • DOI:10.1016/J.BBI.2016.12.014

Inhibiting the NLRP3 inflammasome with MCC950 promotes non-phlogistic clearance of amyloid-β and cognitive function in APP/PS1 mice. — Source link

C. Dempsey, A. Rubio Araiz, Karen Bryson, Orla M. Finucane ...+6 more authors

Institutions: Trinity College, Dublin, University of Queensland

Published on: 01 Mar 2017 - Brain Behavior and Immunity (Academic Press)

Topics: Inflammasome, Caspase 1, Pyroptosis, Neuroinflammation and Microglia

Accepted Manuscript

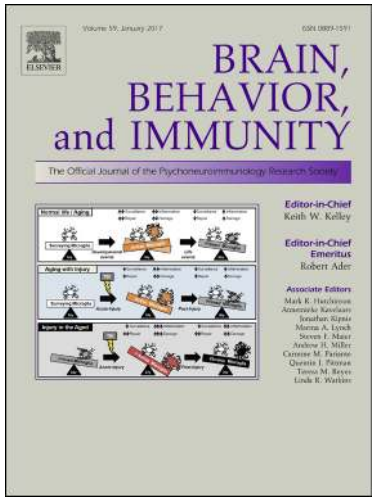

Inhibiting the NLRP3 inflammasome with MCC950 promotes non-phlogistic clearance of amyloid-β and cognitive function in APP/PS1 mice

C. Dempsey, A. Rubio Araiz, K.J. Bryson, O. Finucane, C. Larkin, E.L. Mills, A.A.B. Robertson, M.A. Cooper, L.A.J. O'Neill, M.A. Lynch

PII: S0889-1591(16)30560-8
DOI: http://dx.doi.org/10.1016/j.bbi.2016.12.014
Reference: YBRBI 3046

To appear in: *Brain, Behavior, and Immunity*

Received Date: 3 October 2016
Revised Date: 23 November 2016
Accepted Date: 16 December 2016

Please cite this article as: Dempsey, C., Rubio Araiz, A., Bryson, K.J., Finucane, O., Larkin, C., Mills, E.L., Robertson, A.A.B., Cooper, M.A., O'Neill, L.A.J., Lynch, M.A., Inhibiting the NLRP3 inflammasome with MCC950 promotes non-phlogistic clearance of amyloid-β and cognitive function in APP/PS1 mice, *Brain, Behavior, and Immunity* (2016), doi: http://dx.doi.org/10.1016/j.bbi.2016.12.014

Inhibiting the NLRP3 inflammasome with MCC950 promotes non-phlogistic clearance of amyloid-β and cognitive function in APP/PS1 mice

Abbreviated title: Inflammasome inhibition reduces Aβ in APP/PS1 mice

C. Dempsey[1§], A. Rubio Araiz[1§], K. J. Bryson[1], O. Finucane[1], C. Larkin[1], E. L. Mills[2], A. A. B. Robertson[3], M. A. Cooper[3], L. A. J. O'Neill[2] and M. A. Lynch[1]*

[1]Trinity College Institute for Neuroscience, Trinity College, Dublin 2, Ireland.
[2] School of Biochemistry and Immunology, Trinity Biomedical Sciences Institute, Trinity College, Dublin 2, Ireland.
[3]Institute for Molecular Bioscience, The University of Queensland, Australia.

[§]These authors contributed equally
*Corresponding author
Email: lynchma@tcd.ie

ABSTRACT

Activation of the inflammasome is implicated in the pathogenesis of an increasing number of inflammatory diseases, including Alzheimer's disease (AD). Research reporting inflammatory changes in post mortem brain tissue of individuals with AD and GWAS data have convincingly demonstrated that neuroinflammation is likely to be a key driver of the disease. This, together with the evidence that genetic variants in the NLRP3 gene impacts on

the risk of developing late-onset AD, indicates that targetting inflammation offers a therapeutic opportunity. Here, we examined the effect of the small molecule inhibitor of the NLRP3 inflammasome, MCC950, on microglia *in vitro* and *in vivo*. The findings indicate that MCC950 inhibited LPS+Aβ-induced caspase 1 activation in microglia and this was accompanied by IL-1β release, without inducing pyroptosis. We demonstrate that MCC950 also inhibited inflammasome activation and microglial activation in the APP/PS1 mouse model of AD. Furthermore, MCC950 stimulated Aβ phagocytosis in vitro, and it reduced Aβ accumulation in APP/PS1 mice, which was associated with improved cognitive function. These data suggest that activation of the inflammasome contributes to amyloid accumulation and to the deterioration of neuronal function in APP/PS1 mice and demonstrate that blocking assembly of the inflammasome may prove to be a valuable strategy for attenuating changes that negatively impact on neuronal function.

KEY WORDS: Microglia, interleukin-1β, caspase 1, inflammasome, APP/PS1 mice, Alzheimer's disease, neuroinflammation.

1. INTRODUCTION

Recent GWAS data highlighted the importance of neuroinflammation as a factor that contributes to the pathogenesis of Alzheimer's disease (AD). These findings identified that mutations in genes specific to microglia/myeloid cells confer a significant risk of developing the sporadic form of AD (Karch and Goate, 2015), validating previous evidence that linked increased activation of microglia and production of inflammatory mediators, including interleukin-1β (IL-1β), with AD (Griffin et al., 1989).

Production of IL-1β is primarily dependent on activation of the inflammasome, a complex of cytosolic proteins that assemble in response to **several factors. Among these factors are** reactive oxygen species and also misfolded proteins that trigger lysosomal rupture and cathepsin release (Haneklaus and O'Neill, 2015; Man and Kanneganti, 2015). **Several inflammasomes have been described but the NLRP3 inflammasome is best described,** and its activation is now recognized as a central component in the development of several inflammatory and autoimmune diseases.

Amyloid-β (Aβ) peptide, which accumulates to form the characteristic plaques in AD, activates the NLRP3 inflammasome. It is engulfed by cells and the consequent lysosomal activation and cathepsin B release triggers assembly of the inflammasome, activation of caspase 1 and release of IL-1β (Halle et al., 2008). These data suggested a possible role for the inflammasome in AD and the observation that NLRP3-deficiency in the APP/PS1 mouse model decreased neuroinflammation and Aβ accumulation, and improved neuronal function, supports this hypothesis (Heneka et al., 2013). Notably, expression of several components of the inflammasome, including NLRP3 and caspase 1 as well as IL-1β and IL-18, is increased in monocytes from AD patients, and to a lesser extent from patients with mild cognitive impairment (Saresella et al., 2016). Recent evidence suggests that the rs10754558 variant of the NLRP3 gene confers a significant risk of late-onset AD, particularly in ApoE ε4 carriers and while the rs2027432 variant is also associated with increased risk, the rs35829419 variant (Q705K in *NLRP3*) is associated with protection (Tan et al., 2013).

A recently-described small molecule inhibitor of the NLRP3 inflammasome, MCC950, has been shown to increase survival, and decrease serum IL-18, in a mouse model of cryopyrin-associated periodic syndrome (CAPS) (Coll et al., 2015). **These syndromes are rare, inherited, autoinflammatory diseases that are caused by autosomal-dominant mutations of the NLRP3 gene. They are characterized by systemic inflammation of**

several organs, including brain, as a result of inappropriate cryopyrin-driven inflammasome activation and IL-1β production (Mortimer et al., 2016). MCC950 is a diarylsulphonylurea-containing compound that was originally shown to reduce ATP+LPS-induced mature IL-1β production in monocytes and macrophages; it was recognized that the compounds, which included MCC950 (then called CRID), acted independently of the stimulus (Perregaux et al., 2001).

Coll and colleagues also showed that MCC950 reduced the severity of symptoms in an animal model of multiple sclerosis (Coll et al., 2015). This was attributed to the reduction in IL-1β-induced activation of γδ T cells, and consequently IL-17 production by $CD4^+$ T cells; MCC950 suppressed IL-1β production by dendritic cells and macrophages, which together with IL-23, is required for IL-17 production by γδ and Th17 cells (Sutton et al., 2009).

Here, we investigated the effect of MCC950 in the APP/PS1 mouse model of AD and show that it improves cognitive function and reduces both Aβ accumulation and microglial activation. MCC950 prevented inflammasome activation and IL-1β release from microglia and, at the same time, promoted Aβ phagocytosis. The data suggest that inhibiting NLRP3 inflammasome assembly may be key to limiting the pathology in AD.

2. MATERIALS AND METHODS

Animals

Neonatal C57/BL6 mice were used to prepare cultured microglia. For the in vivo experiments, we used male and female wildtype and APPswe/PS1dE9 mice (hereafter referred to as APP/PS1 mice). This double transgenic mouse model was produced by co-injection into pronuclei of the APP695 isoform containing the Swedish mutation and PS1 with exon-9 deleted. Each gene was under the control of an independent PrP promoter (Jankowsky et al., 2001). All experiments were performed under license from the Health Products Regulatory Authority of Ireland in accordance with EU regulations and with local ethical approval (Trinity College Dublin). Animals were housed under controlled conditions (20-22°C, food and water *ad lib*) and maintained under veterinary supervision.

Treatment schedule

Wildtype and APP/PS1 mice (12 months at the start of the study) were subdivided into MCC950- and control-treated groups **and experiments were carried out in 2 batches, separated by 6 months. The numbers of male and female mice in the wildtype control-treated and MCC950-treated groups were 7 and 4, and the numbers of male and female mice in the APP/PS1 control-treated and MCC950-treated groups were 4 and 7, and 4 and 8 respectively. Details with respect to the production of the preparation of MCC950 used here is described in detail previously (Coll et al., 2015).** Mice received intraperitoneal injections of sterile PBS (control) or MCC950 (10 mg/kg **in PBS**) every second day for 3 months and in the 8th and 9th week of treatment, their performance in a T-maze and a novel object recognition task was assessed. At the end of the 3-month treatment, mice were anaesthetized, transcardially perfused and the brain was removed (Minogue et al., 2014). One half was stored for later preparation of sections for immunohistochemistry, and the hippocampus and cortex were dissected free from the other side of the brain and flash frozen for later analysis.

Behavioural analysis

To assess behaviour in the spontaneous alternation in the T-maze, mice were placed in the start area and allowed to freely explore the left or right arm of the maze. Once a mouse had entered one of the target arms, the door to the arm was closed, the mouse remained in the arm for 30 seconds, after which time the test was repeated with the doors open. Cognitively-healthy mice usually enter the previously-unexplored arm. After each trial the mouse was

placed back in its cage and tested again after all other animals had been evaluated in the task. Successful alternations were recorded over 8 trials.

Prior to testing in the 2-object novel object recognition test, mice were habituated to the open field testing arena for 3 days for 5 min on day 1 and 20 min on days 2 and 3. On the fourth day, mice were allowed to freely explore 2 identical objects in the open field for 10 min (training period) and, after 1h, were returned to the open field with one of the two original objects replaced by a novel object. The mice were allowed to freely explore both objects for 5 min (test period). The time spent exploring the objects was measured. The location preference (to assess the impact of position on preference) is described as the time exploring one object/total time exploring × 100% and the recognition index, assessed in the testing phase, is the time exploring novel object /total time exploring × 100%

Immunohistochemistry

Congo red was used to identify Aβ plaques as previously described (Minogue et al., 2014). Briefly, sagittal sections of hippocampal tissue were equilibrated to room temperature, fixed in ice-cold methanol (5 min), washed, incubated (20 min) in a saturated NaCl solution, and then incubated (2h) in filtered Congo red solution. Slices were washed in dH_2O, counterstained with methyl green solution (1% in dH_2O; 30 sec) and rinsed with running dH_2O for 1 min. Sections were dehydrated by immersion in 95% and subsequently 100% ethanol, incubated in xylene (3 x 5 min) and mounted onto coverslips using dibutyl-phthalate in xylene (DPX) (VWR, US) and allowed to set. Slices were stored at 4°C until required and then imaged using a microscope (Olympus DP72)**. The number of plaques was counted, approximately midway along the rostral-caudal axis, and 9 sections from each animal were examined.**

To assess immunoreactivity of CD11b and CD68, sagittal sections were equilibrated to room temperature, fixed in PFA 4% (30 minutes), washed and incubated (1h) in 10% normal horse serum (NHS) to block non-specific binding and overnight in anti-CD11b or anti-CD68 antibody (AbD Serotec, UK) 1:100 in 10% NHS to block non-specific binding and overnight in anti-CD11b or anti-CD68 antibody (1:100 in 10% NHS; overnight; 4°C. Sections were washed, incubated (1h) with the secondary antibody, washed and incubated (45 min) in ABC solution (Vector labs; US), washed and incubated with DAB. Finally, sections were washed and dehydrated, mounted and stored as described for Congo red staining. To assess caspase 1, sections were incubated at 4°C with the **primary anti-caspase 1 antibody (1:250; raised in goat;** Santa Cruz, US) followed by the Alexa Fluor® 594 donkey anti-goat IgG (1:1000) and mounted in ProLong®Gold with the nuclear marker DAPI (Life Technologies). Images **(6 fields/section; 3 sections from 6 animals per treatment group repeated 3 times on separate days)** were acquired with a Zeiss AX10 Imager A1 microscope at 40X magnification. Analysis of the images was undertaken with ImageJ software.

Preparation of Primary Glial Cultures

Microglia were prepared from neonatal C57/BL6 mice as previously described (Costello et al., 2015). Microglia ($4x10^4$ cells/cm^2 were plated onto coverslips coated with poly-D-lysine (5μg/ml; Merck Millipore Ltd, UK) and, after 48h, were preincubated with LPS (1μg/ml; Enzo Life Sciences, UK). After 4h, MCC950 (100nM) was added followed by the addition of Aβ (10μM; Invitrogen, UK) 30 min later; this concentration was chosen following preliminary data that indicated its near-complete inhibition of LPS+Aβ-induced increase in IL-1β and its lack of effect on IL-6 and TNFα, and also on cytokine mRNA expression. Incubation continued for a further 24h before analysis**. To prepare Aβ, lyophilized $Aβ_{1-40}$ and $Aβ_{1-42}$ peptides (Invitrogen, UK) were dissolved in HPLC grade water to provide a 6mg/ml stock solution, diluted to 1mg/ml using sterile PBS and allowed to aggregate (24 h, 220 rpm, 37°C). This preparation contains both oligomers and fibrils as evidenced by enhanced Thioflavin T binding (data not shown).**

In separate experiments, designed to assess the impact of LPS+ATP on inflammasome activation, cells were preincubated with LPS (1μg/ml) for 2.5h, after which time MCC950 (100μM) was added. Incubation continued for 30 min before addition of ATP (5mM; Sigma, UK) and, after a further 5h, supernatant samples were taken for analysis of IL-1β concentration and LDH activity.

LDH assay

Samples of supernatant were used in an LDH cytotoxicity assay to assess the impact of the different treatments on cell viability. Samples (50μl) or positive control solution (50 μl; supplied by the manufacturer) were incubated (30 min, 37ºC) in 96-well plates, stop solution (50 μl; supplied) was added and absorbance was measured at 490nm, subtracted from absorbance at 680nm, and expressed a percentage of positive control.

Analysis of cytokines by ELISA and RT-PCR

Cytokine concentrations were assessed in supernatant samples from cultured microglia and samples of cortical homogenate as previously described (Minogue et al., 2012). Briefly, 96-well plates (Nunc-Immuno plate with Maxisorp surface, Denmark) were coated with capture antibody (rat anti-mouse IL-1β or goat anti-mouse IL-6 and TNFα antibody (R&D Systems, US) and incubated (overnight, 4ºC). Duplicate samples or standards (50μl/well) were added and plates were incubated (24h, 4ºC) and washed before addition of detection (biotinylated goat anti-mouse) antibody for (1h, room temperature). Plates were washed, incubated with streptavidin-horseradish peroxidase conjugate (20 min, room temperature) and washed before addition of substrate solution (50μl; 1:1 H_2O_2:tetramethylbenzidine; R&D Systems, US). After colour development, the reaction was stopped by adding 1M H_2SO_4 (25μl) and plates were read at 450nm (Labsystem Multiskan RC, UK).

Cytokine mRNA expression was assessed in isolated microglia and hippocampal tissue by RT-PCR as previously described (Costello et al., 2016). **In addition to analysis of cytokines, we also assessed mRNA expression of mannose receptor (MRC1) and arginase 1 (Arg 1) in hippocampal tissue as a measure of M2 activation. The assay ID's for the genes examined were: β-actin (4352341E), IL-1β (Mm00434228_m1), IL-6 (Mm00446190_m1), TNFα (Mm00443258_m1), MRC1 (Mm00485148_m1) and Arg-1 (Mm00475988_m1).**

Detection of soluble Aβ

Snap-frozen cortical tissue was homogenised in sodium dodecyl sulphate (SDS) buffer (1% SDS, 50mM NaCl in dH_2O) containing protease and inhibitors (1%; Sigma-Aldrich, UK) and centrifuged at 21,500 x *g* for 20 minutes at 4°C. **This yields a supernatant that contains the SDS-soluble Aβ and the insoluble material in the pellet. Supernatant samples were normalized for protein and the soluble Aβ concentrations in these samples were** determined using a MULTI-SPOT® Human/Rodent (4G8) Abeta Triplex Ultra-Sensitive Assay (Meso Scale Discovery, USA) as per the manufacturer's instructions. The plate was read using a Mesoscale Sector Imager (Meso Scale Discovery, US) and Aβ concentrations calculated relative to the standard curve.

Confocal image analysis

Microglial cells plated onto poly-D-lysine-coated cover slips were fixed with PFA (4%; 30 min), washed and blocked by incubation with 10% NHS and 0.1% Triton X-100 for 1h and incubated at 4ºC with the primary antibodies anti-Iba1 (Wako, Japan 1:1000) and anti-Aβ (Biolegend, US, 1:500) followed by Alexa Fluor® 594 donkey anti-rabbit IgG (1:1000), Alexa Fluor® 488 donkey anti-mouse IgG (1:1000) and mounted in ProLong®Gold with the nuclear marker DAPI (Thermo Scientific, US). To assess caspase 1 and apoptosis-Associated Speck-Like Protein Containing CARD (ASC), microglia were sequentially incubated anti-caspase-1 raised in goat (Santa Cruz, US 1:100) and ASC (Proteintech, UK, 1:250), Alexa Fluor® 488 chicken anti-rabbit IgG (1:1000) and Alexa

Fluor® 594 donkey anti-goat IgG (1:1000), and mounted as above. Images (10 fields; 40X magnification; triplicate analysis) were acquired with a Zeiss AX10 Imager A1 microscope. Analysis of images was undertaken with ImageJ software; the number of $A\beta^+$ microglia was assessed and colocalization of caspase 1 and ASC was carried out using the specific plug-in Colocalization Finder. Control experiments with each secondary antibody, alone or in combination were included and images were acquired sequentially on a Leica SP8 scanning confocal microscope for each fluorophore to eliminate cross-signal contamination.

Analysis of Aβ engulfment by microglia

For analysis of the effect of IL-1β on phagocytosis, microglia ($4x10^4$ cells/cm^2 were plated onto coverslips coated with poly-D-lysine (5μg/ml; Merck Millipore Ltd, UK). After 48h, cells were preincubated with IL-1β (10ng/ml; Affymetrix eBioscience) for 24h then stimulated for 2h with $A\beta_{1-40}$ (5μM; Invitrogen, UK), pulse centrifuged for 15s in a benchtop microcentrifuge to remove large aggregates. The coverslips were washed 3 times in PBS, fixed in 4% PFA, washed a further 3 times in PBS and stored in PBS at 4°C. The % of Iba^+ cells that engulfed Aβ was calculated by enumerating the total number of Iba^+ cells and the number of Iba^+ $A\beta^+$ cells in 3D projection images generated from Z stacks using a Zeiss Axiovert 200M confocal microscope and processed using LSM Image Browser software**. In total, 402 cells were examined.**

Western immunoblotting

Cultured microglia were lysed (composition in mM: Tris-HCl 10, NaCl 50, $Na_4P_2O_7.H_2O$ 10, NaF 50, 1% Igepal, phosphatase inhibitor cocktail I and II, protease inhibitor cocktail; Sigma, UK), equalized for protein and added to 4x SDS sample buffer (composition: Tris-HCl 100mM, pH 6.8, 4% SDS, 2% bromophenol blue, 20% glycerol; Sigma, UK). Samples were boiled at 100°C for 5 min, aliquots (15-30μg protein) were applied to 15% SDS gels and proteins were transferred to nitrocellulose membrane (Advansta, US) which was blocked in Tris-buffered saline containing 0.05% Tween® 20 (TBS-T) and 5% non-fat dried milk/TBS-T (1h, room temperature). Membranes were incubated overnight at 4ºC with anti-IL-1β (Adipogen, US), **anti-caspase-1 p45/p20 raised in rabbit** (Cell Signaling, US) or anti-β-actin (Sigma, UK) in 3% BSA/TBS-T, washed and incubated with a secondary anti-rabbit, anti-goat or anti-mouse antibody as appropriate (Jackson Immunoresearch, US) in 2% BSA/TBS-T for 1-2h. Immunoreactive bands were detected using WesternBright ECL chemiluminescent substrate (Advansta, US). Images were captured using the Fujifilm LAS-4000 imager and densitometric analysis was carried out using ImageJ (http://rsb.info.nih.gov/).

Statistical analysis

Data are presented as the mean ± SEM. Statistical analysis was carried out using an unpaired Student's *t*-test, or a 2-way ANOVA **and post hoc analysis using the Bonferroni Multiple Comparison test.**

3. RESULTS

Microglia were incubated with LPS and ATP or LPS and Aβ and both stimuli increased release of IL-1β Figure 1A, B) although the effect of LPS+ATP was an order of magnitude greater than LPS+Aβ. MCC950 attenuated the effect of both stimuli and a significant interaction between MCC950 and the inflammasome activators was observed ($(F1,20)=27.13$; $p < 0.0001$, $(F1,8)=15.47$; $p = 0.0043$, respectively) **and post hoc analysis indicated that the significant effects of LPS+ATP or LPS+Aβ (***$p < 0.001$) were attenuated by MCC950 ($^{+++}p < 0.001$ and $^{++}p < 0.01$ respectively).** Analysis of cleaved IL-1β by western immunoblotting revealed a similar LPS+Aβ-induced increase that was

attenuated by MCC950 (Figure 1C). We assessed LDH release as an indicator of cell viability and show that LPS+ATP markedly increased LDH release (Figure 1D); a significant MCC950 x LPS+ATP interaction was observed ((F1,8)=70.51; $p < 0.0001$). **Specifically LPS+ATP significantly increased LDH release (***$p < 0.001$; Bonferroni test) and this was blocked by MCC950 (^{+++}p 0.001). In contrast, LPS+Aβ had no effect on LDH release,** either in the presence or absence of MCC950 (Figure 1E). This indicates that cell death associated with inflammasome assembly is dependent on the stimulus. LPS+Aβ increased TNFα and IL-6 ((F1,8)=59.11; $p < 0.0001$ and ((F1,8)=130.88; $p < 0.0001$, respectively; Figure 1F,G) but MCC950 exerted no modulatory effect on these cytokines **and post hoc analysis confirmed that the significant effects on TNFα and IL-6 ($p < 0.01$ and $p < 0.001$ respectively) were unaffected by MCC950.** Consistent with the LPS+Aβ-induced inflammasome activation, this stimulus also increased the caspase 1^+ **immunoreactivity in microglia and this was inhibited by MCC950; analysis revealed a significant interaction between the treatments ((F1,10)=5.29; $p = 0.044$; Figure 2B) and post hoc analysis revealed that MCC950 significantly decreased the LPS+Aβ-induced change ($^+p < 0.05$).** Similar changes were observed with caspase 1^+ ASC^+ microglia although these did not reach statistical significance (Figure 2C).

We examined the impact of inflammasome assembly on phagocytosis of Aβ. **The image (Figure 3A) shows an Iba^+ microglial cell (with a pink-stained nucleus) that engulfed Aβ (white arrows). Analysis of the mean data** showed that intracellular staining of Aβ in $Iba1^+$ microglia was similar in control-, LPS+Aβ- and MCC950-treated cells, and increased when cells were incubated with LPS+Aβ+MCC950 (Figure 3B); the effect of MCC950 was significant ((F1,12)=7.93; p=0.0156) This indicates that MCC950-associated inhibition of inflammasome assembly increases Aβ engulfment of cells, which is consistent with our finding that IL-1β inhibited phagocytosis of Aβ by microglia ($p < 0.05$; student's t-test for independent means; Figure 3C, D).

If this effect is translated into microglia in vivo and, in particular, microglia in a mouse model of AD, it should result in reduced Aβ accumulation. To assess this, we examined the effect of MCC950 in wildtype and APP/PS1 mice. Aβ-containing plaques (indicated with an arrow) were abundant in the brains of APP/PS1 mice (Figure 4A,B) and treatment with MCC950 reduced plaque numbers (*$p < 0.05$; student's t-test for independent means). Predictably the concentrations **of soluble $Aβ_{1-40}$** and $Aβ_{1-42}$ were increased in tissue from APP/PS1 mice (genotype effects ((F1,41)=146.86; $p < 0.0001$ and ((F1,40)=388.14; $p < 0.0001$, respectively; Figure 4C,D); plaque numbers were attenuated in MCC950-treated APP/PS1 mice and a significant genotype x treatment interaction was observed in the case of $Aβ_{1-40}$ ((F1,41)=6.62; $p = 0.0138$). **Post-hoc analysis indicated that the significant increases in $Aβ_{1-40}$ and $Aβ_{1-42}$ (***$p < 0.001$) were attenuated in MCC950-treated APP/PS1 mice ($p < 0.01$ and $p < 0.05$ respectively). These data are consistent with the proposal that MCC950 increased Aβ phagocytosis *in vivo* as it did *in vitro*. There was no significant gender-related difference in plaque numbers in control mice; the mean (± SEM) value in male APP/PS1 mice was 25.35 (± 6.23) and the value was 26.17 (± 2.21) in female APP/PS1 mice.**

MCC950 also decreased inflammasome activation *in vivo*. Thus IL-1β concentration was increased in cortical tissue from APP/PS1 mice and this was attenuated in MCC950-treated APP/PS1 mice; a significant genotype x treatment interaction was observed ((F1,17)=6.82; $p = 0.0182$; Figure 5A)**. Post hoc analysis indicated that IL-1β concentration was significantly greater in samples from APP/PS1 mice compared with wildtype mice (**$p < 0.01$) and although MCC950 attenuated this increase, it did not reach statistical significance. No gender-related change in IL-1β was observed (data not shown).** IL-1β

mRNA, which was increased in tissue from APP/PS1 mice, was unchanged by MCC950 treatment and the same was true of TNFα mRNA and IL-6 mRNA (Figure 5B-D) and in each of these cases genotype-related changes were observed ((F1,41)=45.02; $p < 0.0001$ for IL-1mRNA, (F1,42)=11.95; $p = 0.0013$ for TNFα and ((F1,42)=32.36; $p < 0.0001$ for IL-6). **Post hoc analysis confirmed that cytokine expression was significantly increased in tissue from control-treated APP/PS1, compared with wildtype, mice (***$p < 0.001$). When mRNA expression of IL-1β, TNFα and IL-6 was assessed by gender, the genotype-related difference was greater in female mice compared with male mice but reached statistical significance only in the case of IL-6 mRNA; the means value in tissue from APP/PS1 control-treated male and female mice were 1.30 (± 0.14, SEM) and 2.29 (± 0.10; $p < 0.05$; ANOVA). The genotype-related increases in inflammatory cytokines, particularly TNFα mRNA, suggest that microglia in the APP/PS1 mice adopt an M1 phenotype as previously described (Jones et al., 2015; Minogue et al., 2014). Analysis of MRC1 and Arg1 as indicators of the M2 activation state revealed no significant genotype- or treatment-related changes (Figure 5C,D) and no gender-related changes were observed (not shown).**

MCC950 also decreased the number of Iba^+ cells that stained for caspase 1 in APP/PS1 mice and statistical analysis indicated that there was a significant interaction between genotype and treatment ((F1,28)=10.74; $p = 0.0028$; Figure 6B). **Post hoc analysis indicated that the effect of MCC950 in APP/PS1 mice was significant ($^{++}p < 0.01$; APP/PS1 control vs APP/PS1+MCC950).**

The evidence also demonstrates that CD11b and CD68 immunoreactivity was increased in APP/PS1 mice compared with wildtype mice (Figure 7A,C) and the genotype-related changes were statistically significant in the case of both markers ((F1,34)=9.72; $p = 0.0037$ for CD11b and (F1,32)=6.67; $p = 0.0146$ for CD68; Figure 7B,D). MCC950 treatment attenuated the genotype-associated changes but a significant interaction between genotype and treatment was observed in the case of CD68 immunoreactivity ((F1,32)=14.25; $p = 0.0007$; Figure 7D). Whereas CD11b and CD68 mRNA expression was significantly increased in tissue from APP/PS1 mice, neither was modified in MCC950-treated APP/PS1 mice (data not shown). **Post hoc analysis indicated that the significant difference in CD11b and CD68 mNRA between control-treated wildtype and APP/PS1 mice (**$p < 0.01$; ***$p < 0.001$) was significantly attenuated in MCC950-treated APP/PS1 mice ($^{+}p < 0.05$; $^{+++}p < 0.001$).**

To evaluate whether these changes were reflected in cognitive function, we assessed spontaneous alternation in the T-maze as a measure of working memory and behaviour in the 2-object novel object recognition test as a measure of recognition memory. APP/PS1 mice performed significantly worse than wildtype mice as measured by the percentage of correct alternations over a number of trails ((F1,18)=8.03; $p = 0.0110$; Figure 8A); the effect was not observed in MCC950-treated APP/PS1 mice and while a significant treatment effect was observed ((F1,18)=4.97; $p = 0.0388$) the genotype x treatment interaction did not reach statistical significance. In the 2-object novel object recognition test, APP/PS1 mice performed significantly worse than wildtype mice as assessed by recognition index (Figure 8B) and treatment with MCC950 significantly attenuated this effect; a significant genotype x treatment interaction was observed ((F1,18)=14.95; $p = 0.0011$). **Post hoc analysis indicated that performance was significantly worse in control-treated APP/PS1 mice compared with wildtype mice (*$p < 0.01$; ***$p < 0.001$) and that MCC950-treated APP/PS1 mice performed significantly better than control-treated APP/PS1 mice ($^{+}p < 0.05$; $^{+++}p < 0.001$).** Mice exhibited no location preference (assessed during the training period; data not shown).

4. DISCUSSION

The significant finding here is that treatment of APP/PS1 mice with the inflammasome inhibitor, MCC950, improves cognitive function and reduces microglial activation and Aβ pathology. The impact of MCC950 on Aβ pathology results from its ability to block production of IL-1β while it promotes Aβ phagocytosis by microglia.

MCC950 inhibits LPS+ATP-induced inflammasome activation in mouse bone marrow derived macrophages and human monocyte-derived macrophages and blood mononuclear cells (Coll et al., 2015) and, here, we report a similar effect in microglia. LPS+ATP markedly decreased microglial viability as indicated by analysis of LDH. In contrast, LPS+Aβ, which also induced inflammasome activation in microglia as previously described (Murphy et al., 2014), is a less potent stimulus and did not affect microglial viability. As might be predicted from an inflammasome inhibitor, MCC950 inhibited the LPS+Aβ-induced IL-1β release but did not affect TNFα or IL-6 release, or IL-1β mRNA (not shown). The evidence suggests that MCC950 blocks assembly of the inflammasome, and this is indicated by its ability to prevent co-localization of caspase 1 and ASC in the microglia. At the same time, MCC950 increased Aβ phagocytosis by microglia.

To evaluate the impact of MCC950 in a model of AD, APP/PS1 mice were treated for 3 months from 12 months, an age at which cognitive changes are evident (Browne et al., 2013) and Aβ plaques are well developed. We show that MCC950 attenuated the genotype-related deficits in 2 tests of cognition, and that this was accompanied by a reduction in Aβ plaque numbers and soluble Aβ concentration reflecting the ability of MCC950 to increase phagocytosis of Aβ. MCC950 also attenuated the genotype-related increase in IL-1β and co-localization of ASC and caspase 1 in Iba 1^{+} cells demonstrating its predicted effect on the inflammasome. Indeed the data suggest that the MCC950-related increase in phagocytosis is a result of its ability to decrease IL-1β since incubating microglia in the presence of IL-1β decreased the phagocytic capability of the cells.

Microglial activation is a well-described characteristic of the brain in AD and in animal models of AD (Heneka et al., 2016; Jones et al., 2015; Minogue et al., 2014) and the genotype-related increases in CD11b and CD68 immunoreactivity reflect this change. MCC950 reduced both markers indicating that it restored this measure of microglial homeostasis, which may be proxy markers of inflammasome activation.

A positive correlation between Aβ pathology and inflammasome activation has been identified by Heneka and colleagues who demonstrated that inflammasome activation occurred in the brain of APP/PS1 mice and that knocking out NLRP3 reduced IL-1β production and amyloid plaque burden (Heneka et al., 2013). This was attributed to the skewing of microglia to an M2-like phenotype in NLRP3-deficient APP/PS1 mice. However, in apparent contrast with this, chronic upregulation of human IL-1β in the hippocampus of APP/PS1 x IL-$1\beta^{XAT}$ mice (Shaftel et al., 2007) and in subiculum of 3xTg x IL-$1\beta^{XAT}$ mice (Ghosh et al., 2013) reduced the Aβ load in these brain areas and this was also attributed to the predominantly M2-like microglia in these mice (Cherry et al., 2015). **In the present study, the evidence suggested that microglia in APP/PS1 mice adopt an inflammatory phenotype as indicated by the increased expression of inflammatory cytokines and no change in MRC1 and Arg1, which are indicative of the M2 phenotype.**

The twin effects of MCC950 in inhibiting IL-1β processing and increasing phagocytosis of Aβ are consistent with evidence that suggests IL-1β may inhibit phagocytosis. An anti-IL-1R blocking antibody has been reported to reduce insoluble $A\beta_{1\text{-}42,}$ fibrillar Aβ oligomers and large Aβ-containing plaques in brain tissue from 3xTg mice (Kitazawa et al., 2011) and IL-$1\beta^{+}$ microglia prepared from APP/PS1 mice had reduced Aβ compared with IL-$1\beta^{-}$ microglia (Saresella et al., 2016). The decrease in brain IL-1β in APP/PS1/$NLRP3^{-/-}$, was also

accompanied by evidence of increased phagocytosis of Aβ by microglia, assessed by evaluating the presence of the amyloid dye methoxy-X04 using flow cytometry (Heneka et al., 2013).

The data point to a potential therapeutic value of MCC950 in AD, adding to evidence of its value in other conditions where inflammation is key (Coll et al., 2015), although it has to be acknowledged that translation of efficacy from an animal model to the human disease is a very significant step. Despite this, MCC950 has undergone some clinical testing as it was originally developed as a treatment for arthritis and it has the advantage that it can be delivered orally. The possibility that it may be useful in early-onset disease is particularly interesting.

5. CONCLUSIONS

Our evidence shows that MCC950, by inhibiting inflammasome activation and increasing phagocytic capability of microglia, reduces Aβ pathology and consequently improves cognition. This identifies inflammasome activation as a contributory factor in driving the pathology and associated loss of function and establishes the inflammasome is an important therapeutic target in AD.

Acknowledgments: The authors gratefully acknowledge funding from Science Foundation Ireland to M.A.L. and L.A.J.O'N. E.L.M was the recipient of an EMBARK post-graduate award from the Irish Research Council (IRCSET G30558). M.A.C. is supported by a NHMRC Professorial Research Fellowship (APP1059354) and A.A.R. is supported by NHMRC Project Grant (APP1086786).

FIGURE LEGENDS

Figure 1. MCC950 attenuates the LPS+Aβ-induced increase in IL-1β without affecting cell viability

Microglia from neonatal mice were incubated with LPS (1μg/ml), MCC950 (100μM) was added at 2.5h and ATP (5mM) at 3h and incubation continued for 5h. Alternatively cells were incubated with LPS (1μg/ml), MCC950 (100μM) was added at 4h and Aβ (10μM) at 4.5h and incubation continued for 24h. Supernatant samples were assessed for cytokines and LDH and also for pro- and cleaved IL-1β by western immunoblotting.

A,B. A significant MCC950 x LPS+ATP interaction ((F1,20)=27.13; $p < 0.0001$), and a significant MCC950 x LPS+Aβ interaction ((F1,8)=14.31; $p = 0.0043$; 2 way ANOVA), was observed. **Post hoc analysis indicated that the significant effects of LPS+ATP or LPS+Aβ (***$p < 0.001$) were attenuated by MCC950 ($^{+++}p < 0.001$ and $^{++}p < 0.01$ respectively).**

C. LPS+Aβ increased cleaved IL-1β and this was attenuated by MCC950 whereas no MCC950-associated effect on pro-IL-1β was observed.

D,E. LPS+ATP increased LDH and this was blocked by MCC950 and there was a significant MCC950 x LPS+Aβ interaction ((F1,8)=70.51; $p < 0.0001$) **and post hoc analysis indicated that the significant effects of LPS+ATP (***$p < 0.001$) was attenuated by MCC950 ($^{+++}p < 0.001$).** LPS+Aβ exerted no effect on LDH either alone or with MCC950.

F,G. LPS+Aβ increased supernatant concentrations of TNFα (F) and IL-6 (G) reflecting significant treatment effects; ((F1,8)=59.11; $p < 0.0001$ and ((F1,8)=130.88; $p < 0.0001$, respectively) **and post hoc analysis revealed significant LPS+Aβ effects (**$p < 0.01$; ***$p < 0.001$) that were not affected by MCC950.**

Data are presented **for 3-6 replicates across 2 separate experiments and samples were assessed in triplicate.**

Figure 2. MCC950 prevents the LPS+Aβ-induced increase in caspase 1^+ ASC^+ microglia
Microglia from neonatal mice were plated on poly-D-lysine-coated coverslips and incubated with LPS (1μg/ml), MCC950 (100μM) was added at 4h and Aβ (10 μM) at 4.5h. Incubation continued for 24h, cells were fixed in 4% PFA and stained for caspase 1 p20 and ASC as described in the methods.
A. Sample images are presented showing confocal fluorescence images (40x) of representative fields stained for caspase1 (red) and ASC (green).
B. Analysis of mean data revealed a significant LPS+Aβ x MCC950 interaction **(*(F1,10)=5.29; p = 0.044) in caspase 1 immunoreactivity and a significant difference between LPS+Aβ-induced changes in the presence and absence of MCC950 (+p < 0.05: Bonferroni test).**
C. Similar changes were evident with caspase 1^+ASC^+ cells but the data did not reach statistical significance. **Values for B and C are means ± SEM (n=3 or 4).**

Figure 3. MCC950 increases Aβ phagocytosis in LPS+Aβ-stimulated microglia
Microglia were prepared as described in the legend for Figure 2. Cells were stained for Iba1 and Aβ as described in the methods. The panel shows confocal fluorescence images at 63X magnification.
A. The sample image shows the presence of Aβ (green) in $Iba1^+$ (red) in a cell that was incubated in LPS+Aβ with MCC950. The insert highlights Aβ uptake by an $Iba1^+$ cell. **The cell nucleus is stained pink and the white arrows indicate Aβ that has been engulfed by the cell, which was verified by confocal imaging.**
B. Analysis of mean data **(n = 4)** revealed a significant effect of MCC950 (§(F1,12)=7.93; p=0.0156). C. Sample images show that Aβ was engulfed by control $Iba1^+$ cells (white arrows), this was reduced in IL-1β-treated cells.
D. Analysis of the mean data **(from a total of 402 cells examined)** indicated that IL-1β significantly decreased the percentage of Iba^+ **cells that stained positively for** Aβ (***p < 0.001; student's t-test for independent means).

Figure 4. MCC950 reduces Aβ pathology in APP/PS1 mice.
Cryostat sections of brain tissue were stained for Aβ plaques using Congo red and Aβ plaque numbers in the hippocampus were quantified.
A. Representative images of Congo red staining in the hippocampus of wildtype and APP/PS1 mice are shown. The red arrows highlight some Aβ plaques.
B. There was a significant reduction in the number of plaques present in the hippocampus of APP/PS1 mice that received MCC950 compared with control-treated APP/PS1 mice (*p < 0.05; student's t-test for independent means). Data **were obtained from 3 slides with 3 sections/slide for each mouse and are means** ± SEM; n=11-13).
C,D. The concentrations of $A\beta_{1\text{-}40}$ (C) and $A\beta_{1\text{-}42}$ (D), assessed by ELISA (see methods) were significantly increased in cortical tissue from APP/PS1, compared with wildtype, mice ($^{+++}$genotype effects ((F1,41)=146.86; p < 0.0001 and ((F1,40)=388.14; p < 0.0001, respectively. Treatment with MCC950 attenuated the genotype-associated changes and a significant genotype x treatment interaction was observed in $A\beta_{1\text{-}40}$ (*(F1,41)=6.62; p = 0.0138). **Post-hoc analysis indicated that the significant increases in $A\beta_{1\text{-}40}$ and $A\beta_{1\text{-}42}$ (***p < 0.001) were attenuated in MCC950-treated APP/PS1 mice (p < 0.01 and p < 0.05 respectively). Values are means ± SEM of 11-13 replicates.**

Figure 5. MCC950 attenuates the genotype-related increase in IL-1β.

A. Homogenate from cortical tissue of control- and MCC950-treated wildtype and APP/PS1 mice was assessed for IL-1β concentration by ELISA. The genotype-related increase in concentration of IL-1β was attenuated in MCC950-treated APP/PS1 mice and a significant genotype x treatment interaction was observed (*(F1,17)=6.82; p = 0.0182. **Post hoc analysis indicated a significant increase in IL-1β in control-treated APP/PS1, compared with wildtype, mice (**p < 0.01) and values are means ± SEM (n = 5-6).**

B-D. The genotype-related increases in mRNA expression of IL-1β ($^{+++}$(F1,41)=45.02; p < 0.0001), TNFα ($^{+++}$ (F1,42)=11.95; p = 0.0013) and IL-6 ($^{+++}$ (F1,42)=32.36; p < 0.0001) were not affected by MCC950 treatment. **Post hoc analysis confirmed that cytokine expression was significantly increased in tissue from control-treated APP/PS1, compared with wildtype, mice (***p < 0.001).**

E,F. No significant genotype- or treatment-related changes were observed in either MRC1 or Arg1 mRNA. For C-F mean values ± SEM of 11-13 samples are presented.

Figure 6. MCC950 decreases caspase 1 in microglia of APP/PS1 mice.

MCC950 decreased the number of Iba^{+} cells that stained positively for caspase 1 in APP/PS1 mice (A) and statistical analysis of the data revealed a significant interaction between genotype and treatment (B; (F1,28)=10.74; p = 0.0028) **and post hoc analysis indicated a significant difference between the APP/PS1 control and APP/PS1+MCC950 treatment groups ($^{++}$p < 0.01; n=8).**

Figure 7. MCC950 attenuates the genotype-related increases in microglial activation.

Sections of brain tissue were assessed for CD11b and CD68 immunoreactivity.

CD11b immunoreactivity (A,B) and CD68 immunoreactivity (C,D) were markedly increased in sections from control-treated APP/PS1 mice compared with wildtype mice and significant genotype changes were observed ((F1,34)=9.72; p = 0.0037 for CD11b and ((F1,32)=6.67; p = 0.0146 for CD68). A significant interaction between genotype and treatment was observed in CD68 immunoreactivity (***(F1,32)=14.25; p = 0.0007). **Post hoc analysis indicated that the significant difference in CD11b and CD68 mNRA between control-treated wildtype and APP/PS1 mice (**p < 0.01; ***p < 0.001) was significantly attenuated in MCC950-treated APP/PS1 mice ($^{+}$p < 0.05; $^{+++}$p < 0.001). Data in B and D are means ± SEM (n=12).**

Figure 8. MCC950 improves cognitive function.

Control- and MCC950-treated wildtype and APP/PS1 mice were assessed spontaneous alternation in the T-maze, where performance was assessed by the number of correct alternations made over 8 trials, and for performance in a 2-object novel object recognition test where the ability of mice to recognize a novel object was assessed by the time spent exploring this, compared with a familiar, object.

A. Control-treated APP/PS1 mice performed significantly worse in the spontaneous alternation test than wildtype mice ($^{+}$genotype effect: (F1,18)=8.03; p = 0.0110) but MCC950-treated APP/PS1 mice were significant better (treatment effect: (F1,18)=4.97; p = 0.0388). **Post hoc analysis indicated that performance was significantly worse in control-treated APP/PS1 mice compared with wildtype mice (*p < 0.01) and that MCC950 significantly attenuated the effect of genotype ($^{+}$p < 0.05).**

B. Recognition index was used as an indicator of the relative time mice spent exploring a novel, compared with a familiar, object. This value was reduced in control-treated APP/PS1, compared with wildtype, mice and a significant genotype x treatment interaction was observed (**(F1,18)=14.95; p = 0.0011). **Post hoc analysis indicated that performance was significantly poorer in control-treated APP/PS1 mice compared with control-**

treated wildtype mice (*p < 0.001) and that MCC950 treatment improved performance in APP/PS1 mice ($^{+++}$p < 0.001). Data are presented as means ± SEM (n = 4-6).**

Conflict of Interest: The authors declare no competing conflicts of interest including financial interests.

REFERENCES

Browne, T.C., McQuillan, K., McManus, R.M., O'Reilly, J.A., Mills, K.H., Lynch, M.A., 2013. IFN-gamma Production by amyloid beta-specific Th1 cells promotes microglial activation and increases plaque burden in a mouse model of Alzheimer's disease. J Immunol 190, 2241-2251.

Cherry, J.D., Olschowka, J.A., O'Banion, M.K., 2015. Arginase 1+ microglia reduce Abeta plaque deposition during IL-1beta-dependent neuroinflammation. J Neuroinflammation 12, 203.

Coll, R.C., Robertson, A.A., Chae, J.J., Higgins, S.C., Munoz-Planillo, R., Inserra, M.C., Vetter, I., Dungan, L.S., Monks, B.G., Stutz, A., Croker, D.E., Butler, M.S., Haneklaus, M., Sutton, C.E., Nunez, G., Latz, E., Kastner, D.L., Mills, K.H., Masters, S.L., Schroder, K., Cooper, M.A., O'Neill, L.A., 2015. A small-molecule inhibitor of the NLRP3 inflammasome for the treatment of inflammatory diseases. Nat Med 21, 248-255.

Costello, D.A., Carney, D.G., Lynch, M.A., 2015. alpha-TLR2 antibody attenuates the Abeta-mediated inflammatory response in microglia through enhanced expression of SIGIRR. Brain Behav Immun 46, 70-79.

Costello, D.A., Keenan, K., McManus, R.M., Falvey, A., Lynch, M.A., 2016. The age-related neuroinflammatory environment promotes macrophage activation, which negatively impacts synaptic function. Neurobiol Aging 43, 140-148.

Ghosh, S., Wu, M.D., Shaftel, S.S., Kyrkanides, S., LaFerla, F.M., Olschowka, J.A., O'Banion, M.K., 2013. Sustained interleukin-1beta overexpression exacerbates tau pathology despite reduced amyloid burden in an Alzheimer's mouse model. J Neurosci 33, 5053-5064.

Griffin, W.S., Stanley, L.C., Ling, C., White, L., MacLeod, V., Perrot, L.J., White, C.L., 3rd, Araoz, C., 1989. Brain interleukin 1 and S-100 immunoreactivity are elevated in Down syndrome and Alzheimer disease. Proc Natl Acad Sci U S A 86, 7611-7615.

Halle, A., Hornung, V., Petzold, G.C., Stewart, C.R., Monks, B.G., Reinheckel, T., Fitzgerald, K.A., Latz, E., Moore, K.J., Golenbock, D.T., 2008. The NALP3 inflammasome is involved in the innate immune response to amyloid-beta. Nat Immunol 9, 857-865.

Haneklaus, M., O'Neill, L.A., 2015. NLRP3 at the interface of metabolism and inflammation. Immunol Rev 265, 53-62.

Heneka, M., Andreasson, K.I., Bachstetter, A.D., Colonna, M., Ginhoux, F., Holmes, C., Lamb, B., Landreth, G., Lee, D.C., Low, D., Lynch, M.A., Monsonego, A., O'Banion, M.K., Pekny, M., Puschmann, T., Russek-Blum, N., Sandusky, L.A., Selenica, M.B., Takata, K., Teeling, J., Town, T., Van Eldik, L.J., Schulz, J.B., 2016. Targeting innate immunity for neurodegenerative disorders of the central nervous system. J Neurochem.

Heneka, M.T., Kummer, M.P., Stutz, A., Delekate, A., Schwartz, S., Vieira-Saecker, A., Griep, A., Axt, D., Remus, A., Tzeng, T.C., Gelpi, E., Halle, A., Korte, M., Latz, E., Golenbock, D.T., 2013. NLRP3 is activated in Alzheimer's disease and contributes to pathology in APP/PS1 mice. Nature 493, 674-678.

Jankowsky, J.L., Slunt, H.H., Ratovitski, T., Jenkins, N.A., Copeland, N.G., Borchelt, D.R., 2001. Co-expression of multiple transgenes in mouse CNS: a comparison of strategies. Biomol Eng 17, 157-165.

Jones, R.S., Minogue, A.M., Fitzpatrick, O., Lynch, M.A., 2015. Inhibition of JAK2 attenuates the increase in inflammatory markers in microglia from APP/PS1 mice. Neurobiol Aging 36, 2716-2724.

Karch, C.M., Goate, A.M., 2015. Alzheimer's disease risk genes and mechanisms of disease pathogenesis. Biol Psychiatry 77, 43-51.

Kitazawa, M., Cheng, D., Tsukamoto, M.R., Koike, M.A., Wes, P.D., Vasilevko, V., Cribbs, D.H., LaFerla, F.M., 2011. Blocking IL-1 signaling rescues cognition, attenuates tau pathology, and restores neuronal beta-catenin pathway function in an Alzheimer's disease model. J Immunol 187, 6539-6549.

Man, S.M., Kanneganti, T.D., 2015. Regulation of inflammasome activation. Immunol Rev 265, 6-21.

Minogue, A.M., Barrett, J.P., Lynch, M.A., 2012. LPS-induced release of IL-6 from glia modulates production of IL-1 beta in a JAK2-dependent manner. J Neuroinflammation 9, 126.

Minogue, A.M., Jones, R.S., Kelly, R.J., McDonald, C.L., Connor, T.J., Lynch, M.A., 2014. Age-associated dysregulation of microglial activation is coupled with enhanced blood-brain barrier permeability and pathology in APP/PS1 mice. Neurobiol Aging 35, 1442-1452.

Mortimer, L., Moreau, F., MacDonald, J.A., Chadee, K., 2016. NLRP3 inflammasome inhibition is disrupted in a group of auto-inflammatory disease CAPS mutations. Nature Immunology 17, 1176-+.

Murphy, N., Grehan, B., Lynch, M.A., 2014. Glial uptake of amyloid beta induces NLRP3 inflammasome formation via cathepsin-dependent degradation of NLRP10. Neuromolecular medicine 16, 205-215.

Perregaux, D.G., Mcniff, P., Laliberte, R., Hawryluk, N., Peurano, H., Stam, E., Eggler, J., Griffiths, R., Dombroski, M.A., Gabel, C.A., 2001. Identification and characterization of a novel class of interleukin-1 post-translational processing inhibitors. Journal of Pharmacology and Experimental Therapeutics 299, 187-197.

Saresella, M., La Rosa, F., Piancone, F., Zoppis, M., Marventano, I., Calabrese, E., Rainone, V., Nemni, R., Mancuso, R., Clerici, M., 2016. The NLRP3 and NLRP1 inflammasomes are activated in Alzheimer's disease. Mol Neurodegener 11, 23.

Shaftel, S.S., Kyrkanides, S., Olschowka, J.A., Miller, J.N., Johnson, R.E., O'Banion M, K., 2007. Sustained hippocampal IL-1beta overexpression mediates chronic neuroinflammation and ameliorates Alzheimer plaque pathology. J Clin Invest 117, 1595-1604.

Sutton, C.E., Lalor, S.J., Sweeney, C.M., Brereton, C.F., Lavelle, E.C., Mills, K.H., 2009. Interleukin-1 and IL-23 induce innate IL-17 production from gammadelta T cells, amplifying Th17 responses and autoimmunity. Immunity 31, 331-341.

Tan, M.S., Yu, J.T., Jiang, T., Zhu, X.C., Wang, H.F., Zhang, W., Wang, Y.L., Jiang, W., Tan, L., 2013. NLRP3 polymorphisms are associated with late-onset Alzheimer's disease in Han Chinese. J Neuroimmunol 265, 91-95.

Figure 1

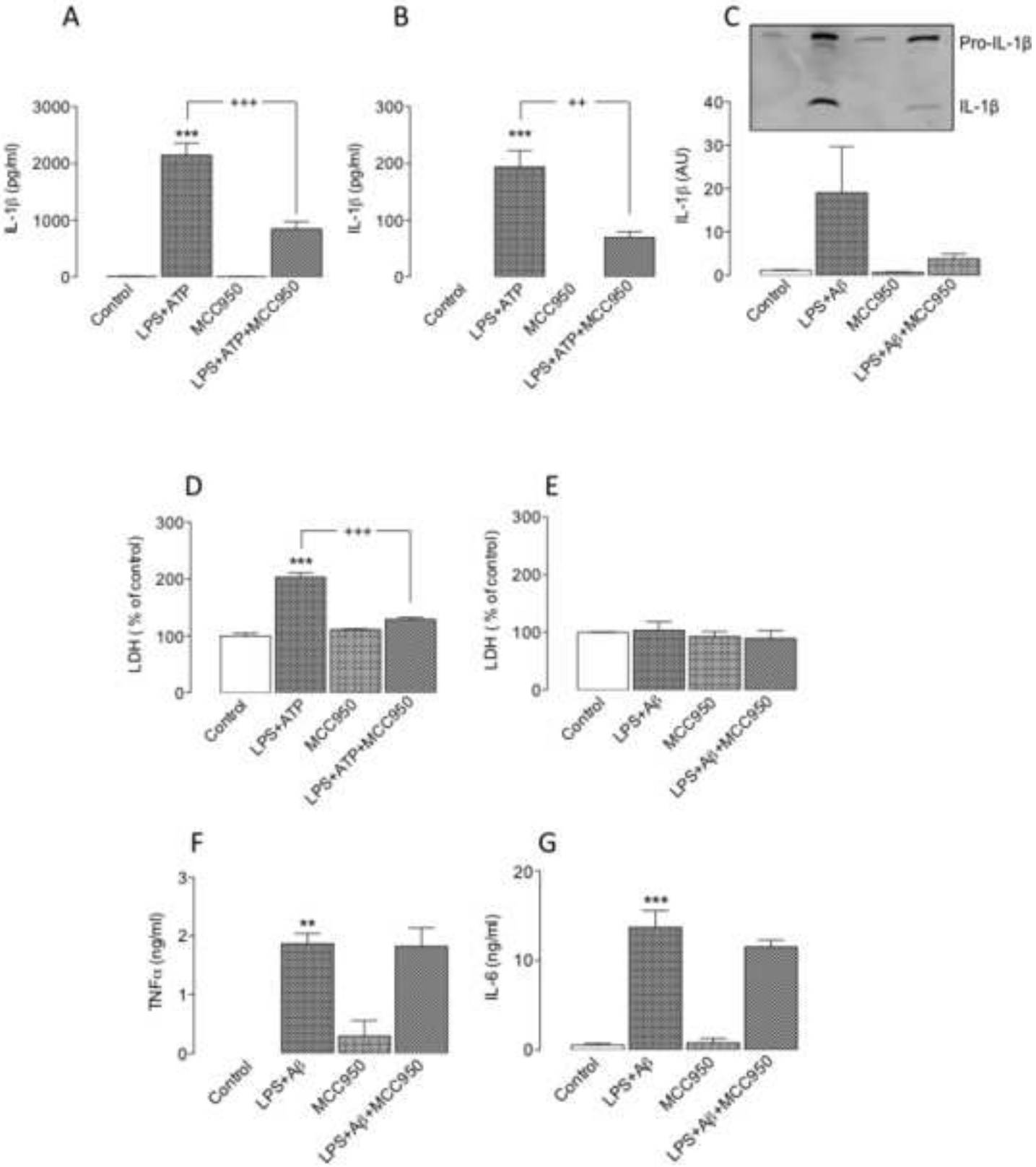

Figure 2

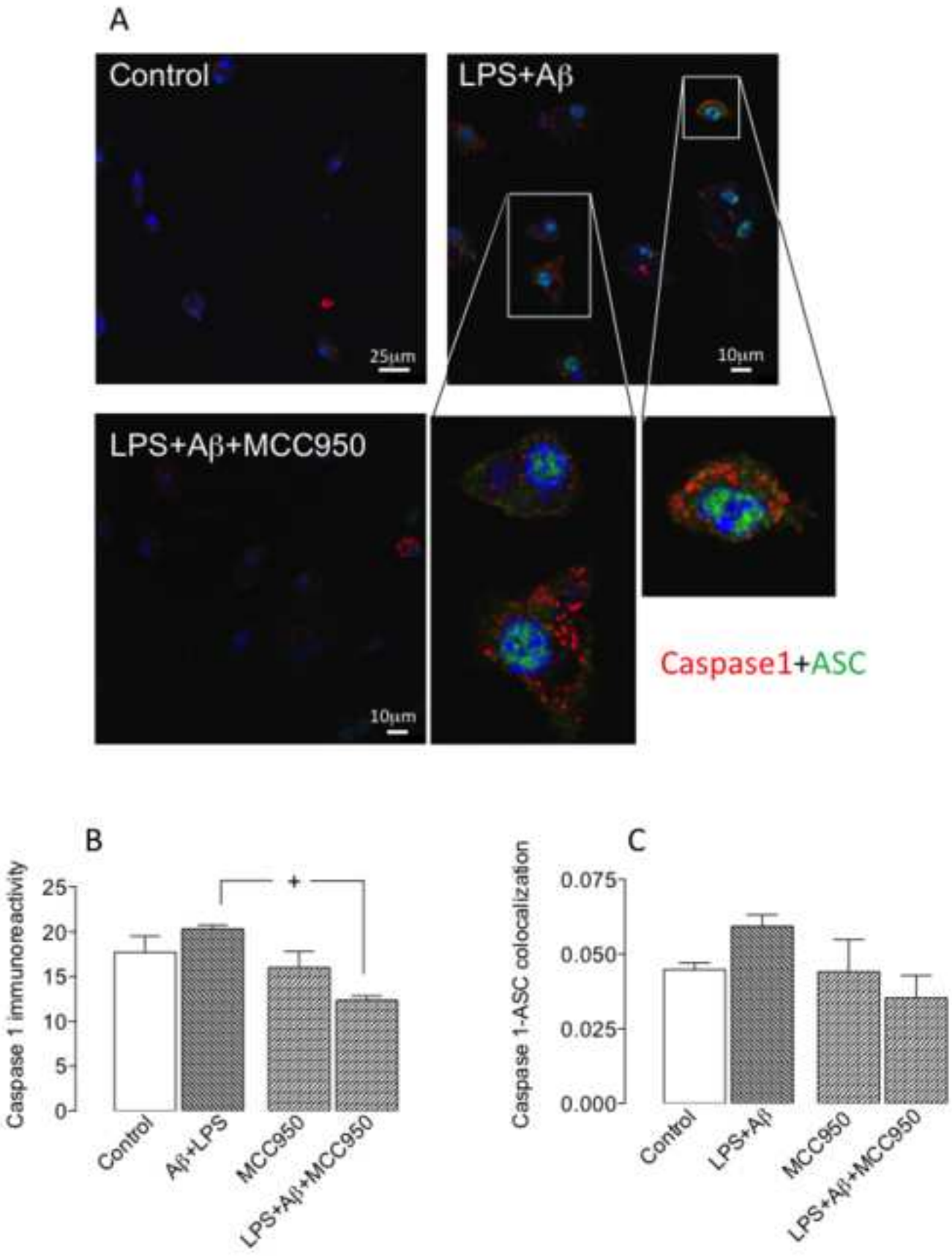

Figure 3

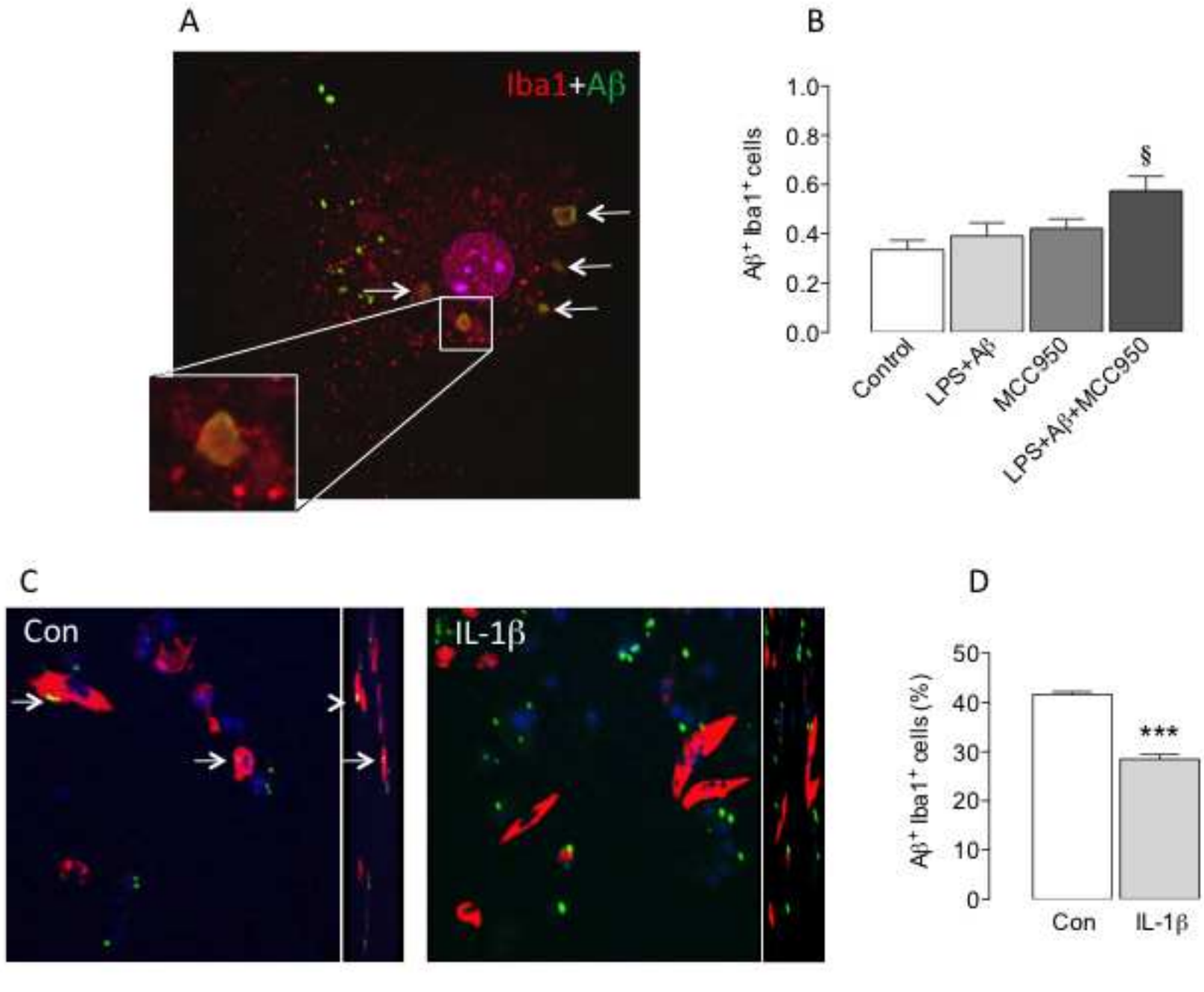

Figure 4

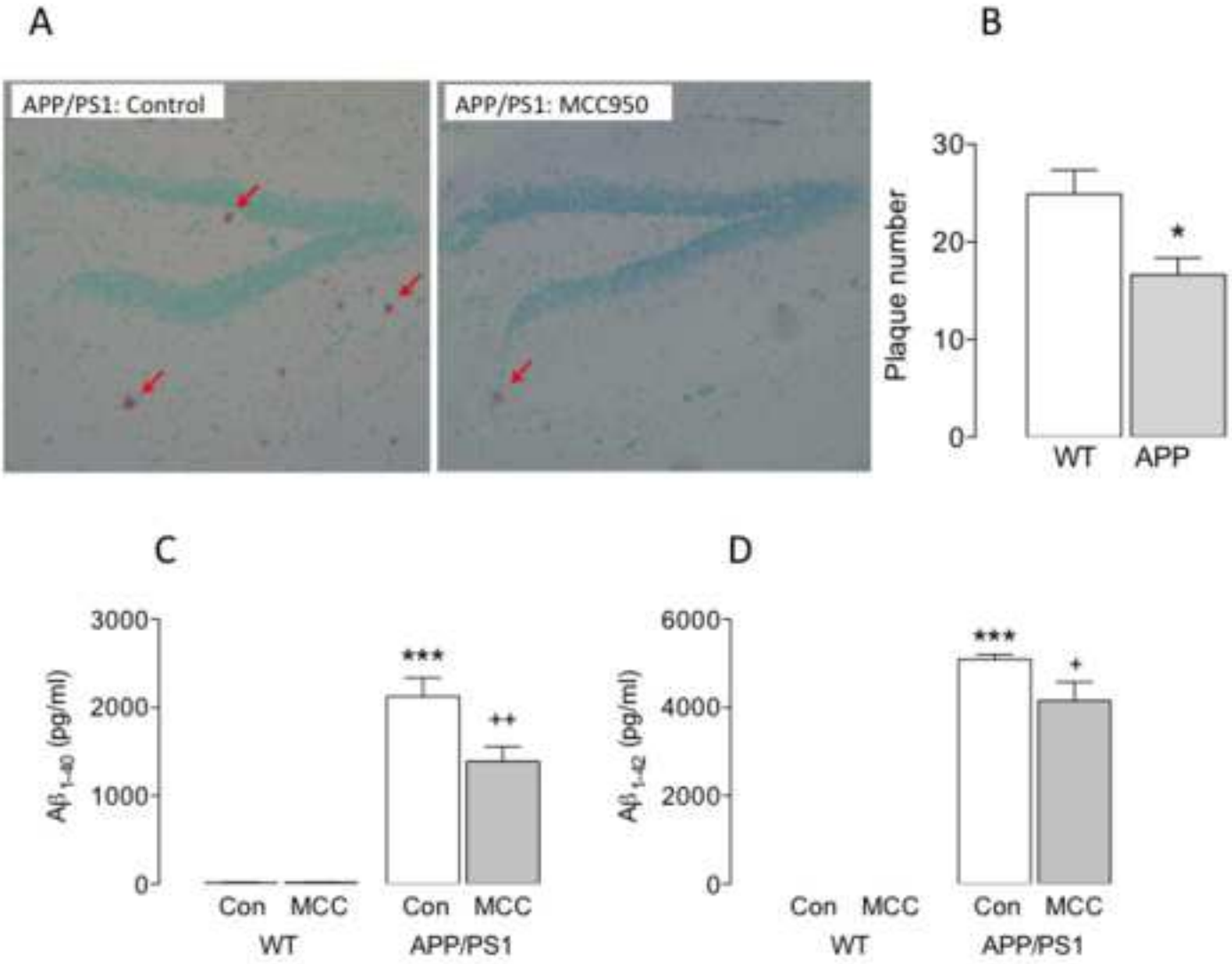

Figure 5

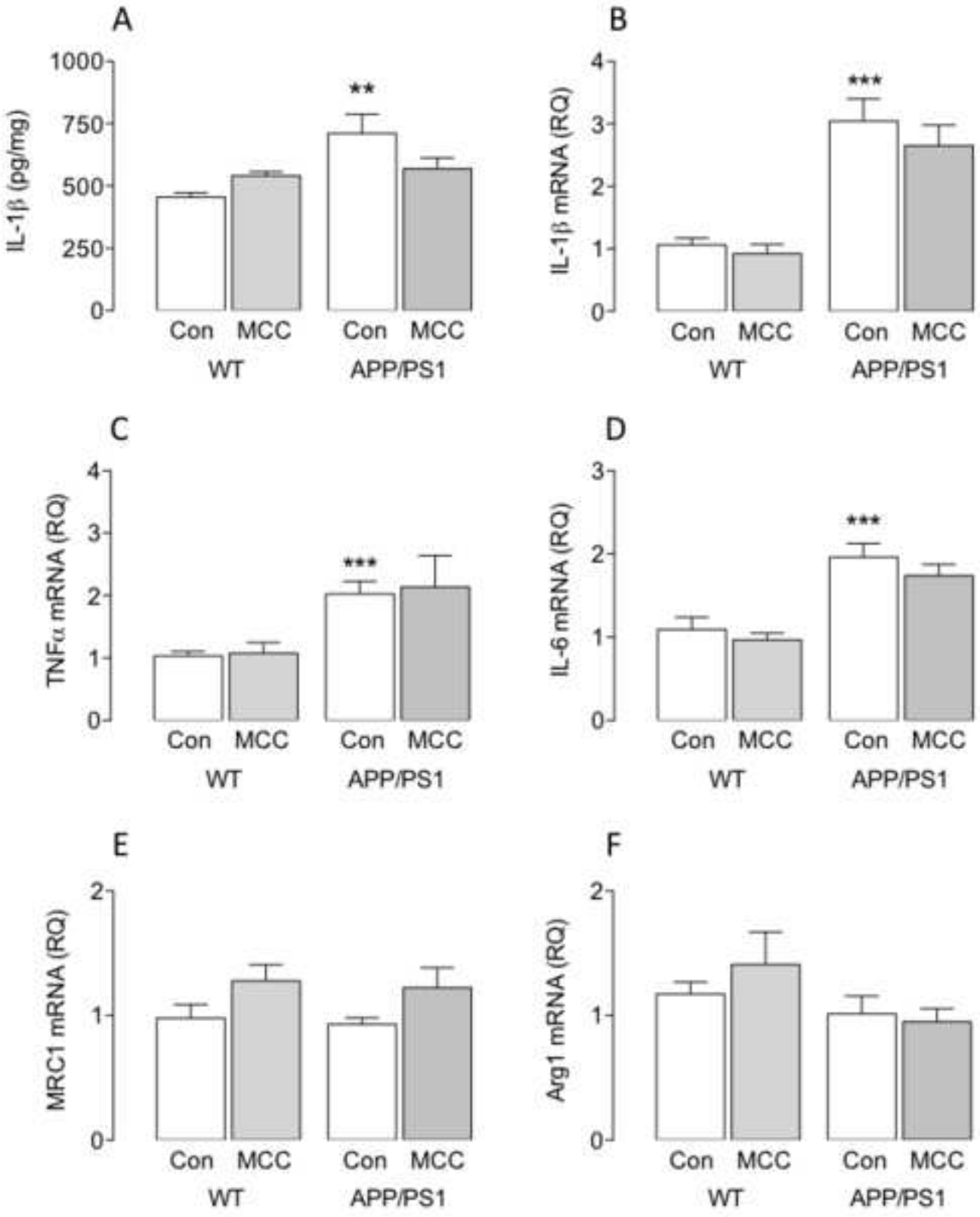

Figure 6

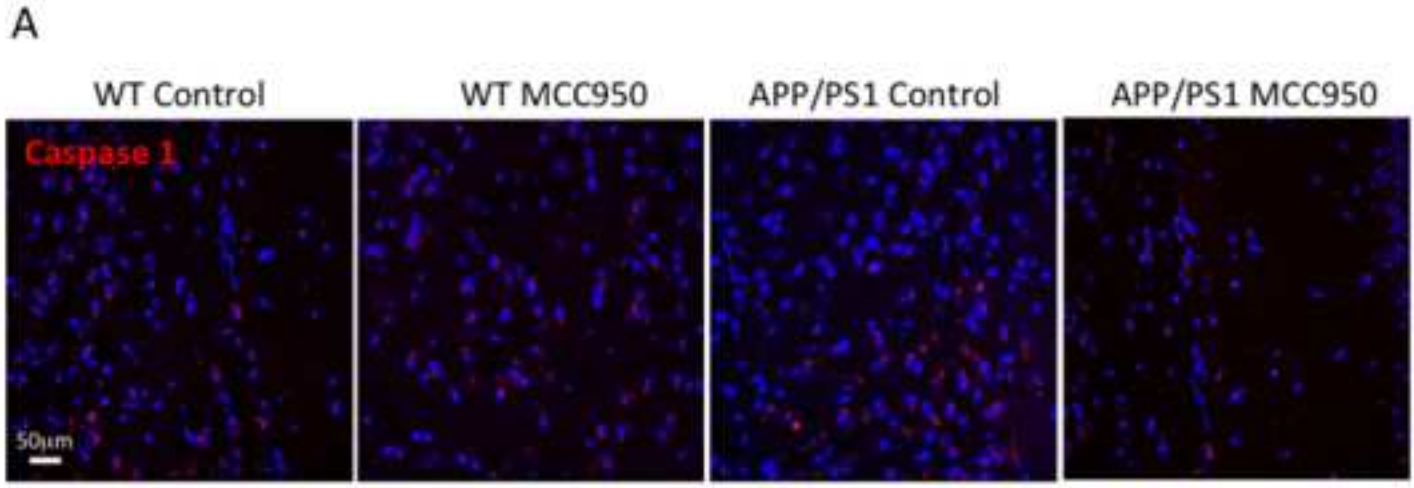

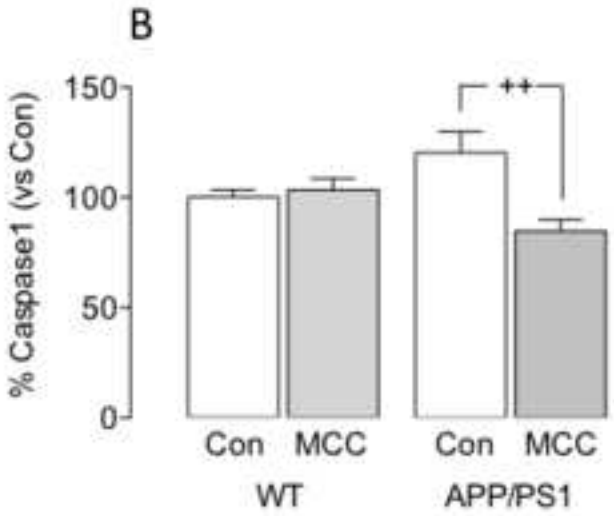

Figure 7

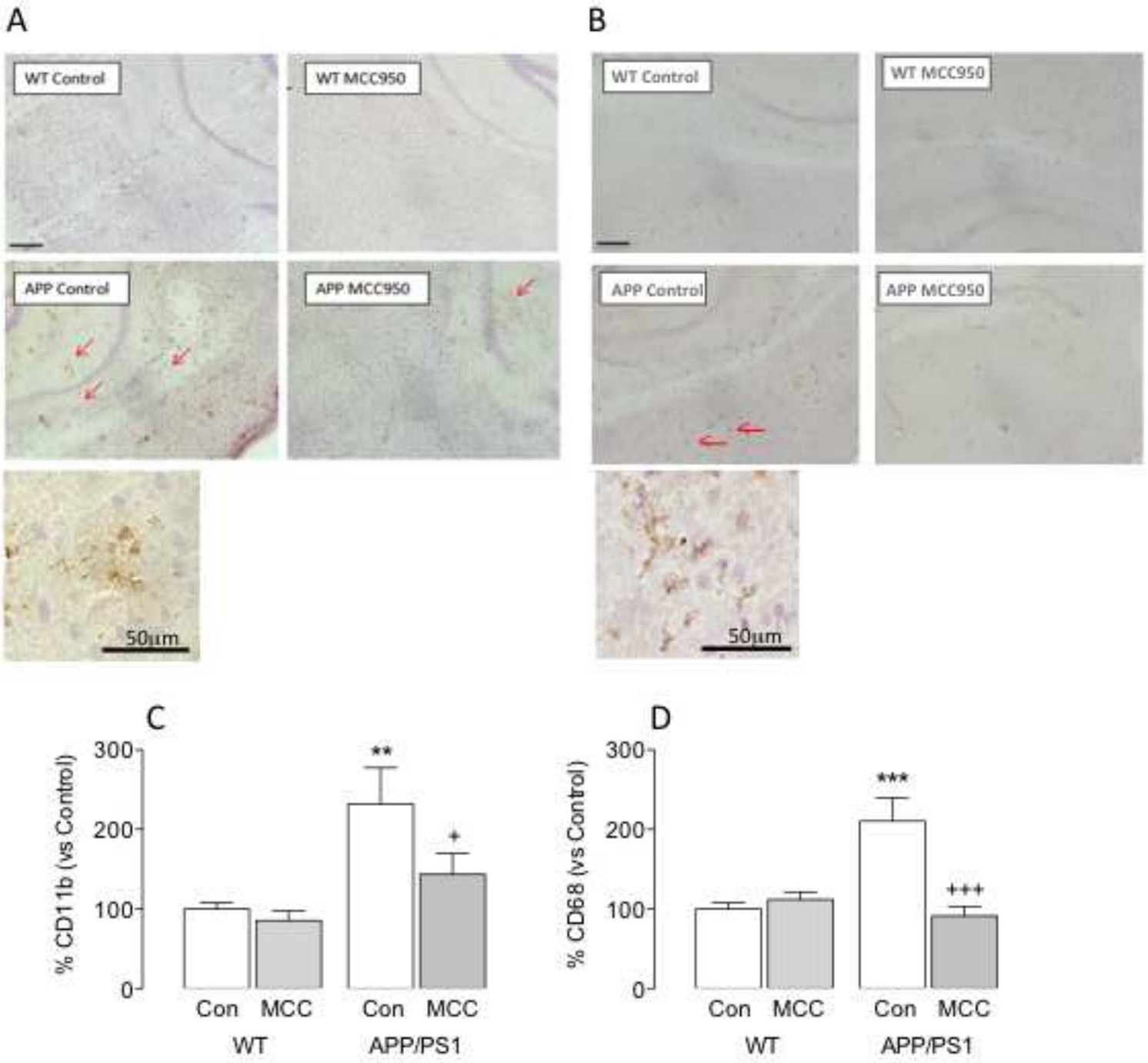

Figure 8

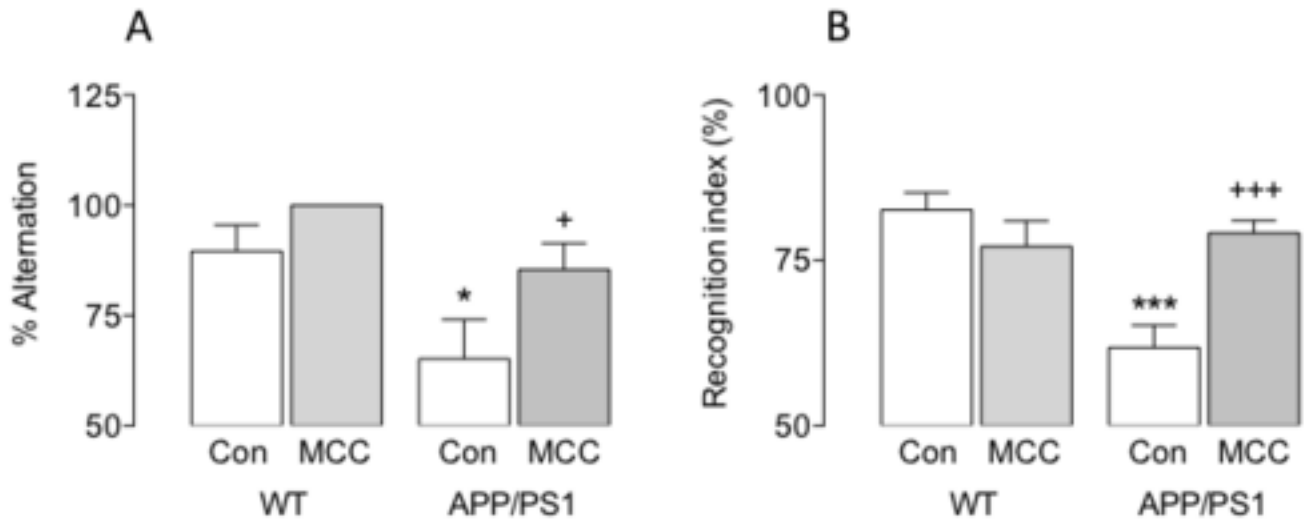

Highlights

- The small molecule inhibitor of the inflammasome, MC950, attenuates Aβ+LPS-induced inflammasome activation in microglia.
- It increases phagocytosis of Aβ by microglia in vitro
- Oral administration of MC950, reduces Aβ accumulation in APP/PS1 mice
- This is accompanied by improved cognitive function and decreased neuroinflammation